Original Research

Quantification of White Matter and Gray Matter Volumes from Three-Dimensional Magnetic Resonance Volume Studies Using Fuzzy Classifiers

R. Craig Herndon, PhD • Jack L. Lancaster, PhD • Jay N. Giedd, MD • Peter T. Fox, MD

We accurately measured white matter (WM) and gray matter (GM) from three-dimensional (3D) volume studies, using a fuzzy classification technique. The new segmentation method is a modification of a recently published method developed for T1 parametric images. 3D MR images were transformed into pseudo forms of T1 parametric images and segmented into WM and GM voxel fraction images with a set of standardized fuzzy classifiers. This segmentation method was validated with synthesized 3D MR images as phantoms. These phantoms were developed from cryosectioned human brain images located in the superior, middle, and inferior regions of the cerebrum. Phantom volume measurements revealed that, generally, the difference between measured and actual volumes was less than 3% for 1.5-mm simulated brain slices. The average cerebral GM/WM ratio calculated from 3D MR studies in four subjects was 1.77, which compared favorably with the estimate of 1.67 derived from anatomical data. Results indicate that this is an accurate and rapid method for quantifying WM and GM from T1-weighted 3D volume studies.

Index terms: Brain MR • Volume measurement • Image processing

JMRI 1998; 8:1097–1105

Abbreviations: WM = white matter, GM = gray matter, 3D = three-dimensional, 2D = two-dimensional, DE = dual echo, CSF = cerebrospinal fluid, PDW = proton density-weighted, T2W = T2-weighted, FCs = fuzzy classifiers, ROIs = regions of interest, T1W = T1-weighted, SPGR = spoiled-gradient-recalled echo-pulse sequence, SNR = signal-to-noise ratio, VF = voxel fraction, T1ρ = pseudo-T1.

From the Department of Radiology and Research Imaging Center, The University of Texas Health Science Center at San Antonio, San Antonio, Texas, and Child Psychiatry Branch (J.N.G.), National Institute of Mental Health, Bethesda, Maryland. Received June 3, 1997; revision requested December 30; revision received January 21, 1998; accepted February 23. Research support was provided by the Human Brain Project, which is funded jointly by National Institute of Mental Health, and National Institute of Drug Abuse (P20 MH/DA52176). **Address reprint requests to:** R.C.H. (BRS, 1633 Babcock, Box 260, San Antonio, TX 78229).

© ISMRM, 1998

BRAIN TISSUE SEGMENTATION techniques have commonly been applied to images acquired by using two-dimensional (2D) MR acquisition techniques (1–15). Neuroimaging researchers can use these brain tissue segmentation methods to assess quantitatively, across a population, both normal and abnormal brain variations. The most common of these segmentation techniques is multispectral analysis (1–9). Multispectral analysis uses 2D dual-echo (DE) MR studies. DE acquisitions, consisting of proton-density weighted (PDW) and T2-weighted (T2W) images, are used because they are spatially registered and provide distinct parameters or features that can be used to define the multispectral space needed for cluster analysis. Clarke et al (16) reviewed numerous classification schemes, including multispectral analysis, for segmenting brain tissues. Many classification methods, including multispectral analysis, use some form of fuzzy classification (5,8–15). Fuzzy classification, in contrast to crisp or hard classification, subdivides the contents of a voxel's volume into different tissue classes. Therefore, fuzzy classifiers can better model a critical physical limitation of imaging, partial volume averaging, that confounds the segmentation process. The research presented in this paper is based upon a recently reported fuzzy classification method used to measure white matter (WM) and gray matter (GM) volumes with T1 parametric images (15).

Previously, WM and GM fuzzy classifiers (FCs) were designed that modeled the fuzziness inherent in the WM/GM and GM/cerebrospinal fluid (CSF) boundaries in T1 parametric images by modeling partial volume effects due to slice thickness and intrinsic tissue inhomogeneities (15). A single standard set of FCs was used to quantify brain tissue volumes from the entire population of subjects. Image data were adapted to the standard fuzzy classifiers instead of the classifiers being adapted to the data. Results from phantom image measurements supported this adaptive scheme (15). The integration of this adaptive scheme with partial volume accommodation resulted in a process whereby the standardized FCs could be used to rapidly and accurately segment WM and GM structures.

The research presented in this paper was motivated by the desire to adapt the standard T1 classification method

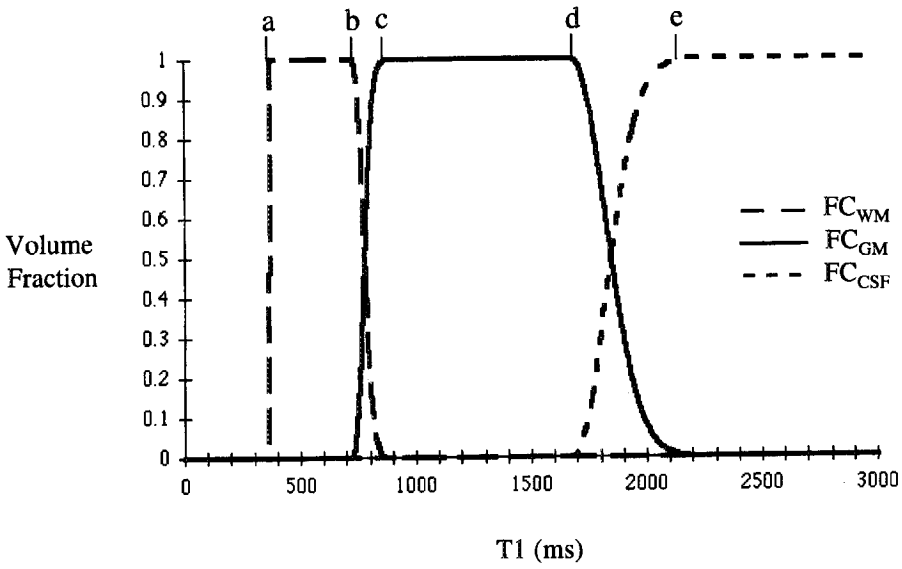

Figure 1. Fuzzy classifiers designed to quantify WM, GM, and CSF in normalized 1.5-mm T1 images. The normalization process adapts image data from different subjects to this standard set of fuzzy classifiers.

to work with T1-weighted (T1W) 3D volume images. For this study, WM and GM volumes were quantified from images acquired with a 3D spoiled-gradient-recalled echo-pulse sequence (SPGR). The 3D SPGR volume acquisition mode was selected for volume quantification because it provided good WM/GM contrast, and the spatially contiguous 1.5 × 0.9375 × 0.9375 mm^3, voxels greatly reduced partial volume-averaging effects at tissue boundaries, compared with 5-mm-thick conventional spin-echo images. The results of this 3D SPGR segmentation method were validated in three different ways. The first validation method was a comparison of calculated and known volumes, using phantom data. In this paper, "phantoms" refer to synthesized MR images of the brain, not physical objects. The second validation was a comparison of human brain tissue volumes measured from 1.5-mm-thick 3D SPGR images to volumes measured from the same individual by a previously published method that works with 5-mm-thick T1-calculated images (15). The third validation was a comparison of WM and GM volumes measured from MR images to WM and GM volumes acquired from anatomical studies.

• MATERIALS AND METHODS

Fuzzy Classifiers for 3D Volume Acquisitions

FCs were modeled as a combination of hard classifiers bounded by half-Gaussian functions. The hard classifiers model the intrinsic inhomogeneity of brain tissues and the half-Gaussians model the partial volume averaging that occurs at the WM/GM and GM/CSF interfaces (Fig. 1). Previously, FCs were developed for only 1-, 3-, and 5-mm slices (15). The same procedures were used to develop the 1.5-mm FCs required for this study. Parameters μ (mean of the half-Gaussian fits) and σ (standard deviation of the half-Gaussians) from the 1- and 3-mm FCs (Table 1) were used as initial values for development of the 1.5-mm FCs with T1 phantom images. Development of the FCs was an iterative process (varying both μ and σ) that minimized the difference between the measured and known phantom volumes. FCs have been developed for 1-, 1.5-, 2-, 3-, and 5-mm slices. These FCs and the templates used to make the phantom images are at our web site[1]. FCs can be developed for slice thicknesses not available by linearly interpolating between parameters from two adjacent FCs.

This classification method uses FCs designated as FC_{WM}, FC_{GM}, and FC_{CSF} in Equations [1] through [3] to segment WM, GM, and CSF. The 1.5-mm CSF FC of Figure 1 was calculated by subtracting the upper half-Gaussian of the 1.5-mm GM FC from unity, as shown in Equations [2] and [3].

$$\begin{aligned} FC_{WM}(T1) &= 0; && T1 < a \\ &= 1; && a \le T1 < b \\ &= \exp[-(T1-\mu)^2/\sigma^2]; && b \le T1 < c \\ &= 0; && T1 \ge c \end{aligned} \quad [1]$$

$$\begin{aligned} FC_{GM}(T1) &= 0; && T1 < b \\ &= 1 - FC_{WM}(T1); && b \le T1 < c \\ &= 1; && c \le T1 < d \\ &= \exp[-(T1-\mu)^2/\sigma^2]; && d \le T1 < e \\ &= 0; && T1 \ge e \end{aligned} \quad [2]$$

$$\begin{aligned} FC_{CSF}(T1_p) &= 0; && T1 < d \\ &= 1 - FC_{GM}(T1_p); && d \le T1 < e \\ &= 1; && T1 \ge e \end{aligned} \quad [3]$$

where *a*, *b*, *c*, *d*, and *e* are parameters in the mathematical models of the FCs. These parameters are the end points for the half-Gaussian models that consist of WM, GM, and CSF FCs. For example, end-point *d* is the largest GM T1 value with unity membership in the GM FC, whereas, *e* is the largest GM T1 value with non-zero membership in the GM FC. The end-point parameters for the 1.5-mm WM and GM FCs (*a*, *b*, *c*, *d*, and *e*) are illustrated in Figure 1 and listed in Table 1. In addition, endpoint parameters for the 1-, 3-, and 5-mm FCs are also listed.

[1] Binary template images of WM, GM, and CSF used for building phantom images are available for download at http://ric.uthscsa.edu/projects.

Table 1
White Matter and Gray Matter Fuzzy Classifier Parameters for Equations 1 and 2

FCl(T1)	m	s	a	b	c	d	e
WM at 5 mm	700	128	370	710	1080		
WM at 3 mm	720	83	370	730	970		
WM at 1.5 mm	730	55	370	740	900		
WM at 1 mm	740	42	370	750	860		
GM at 5 mm	1240	575		710	1080	1250	2990
GM at 3 mm	1400	545		730	970	1410	2770
GM at 1.5 mm	1680	200		740	900	1690	2290
GM at 1 mm	1780	100		750	860	1790	2090

Note.—All T1 values are in milliseconds. m = half-Gaussian mean. s (standard deviation) defines the extent of the half-Gaussian fits. a–e are boundary parameters for the optimized WM and GM fuzzy classifiers.

Pseudo-T1 Parametric Space

The previously reported fuzzy classification method used T1 parametric data (15). Calculating T1 parametric images directly from a single 3D SPGR MR study is not possible; however, a mathematical transformation was used to map 3D SPGR images to approximate forms of T1 parametric images. This transformation enables the application of the standard FCs to the 3D SPGR volume images.

Images are transformed with an analytic solution to Bloch's equations for the SPGR pulse sequence (Equation [4]) (17). Equation [4] is used to approximate the MR signal for a SPGR pulse sequence given the acquisition parameters (TR, TE, and θ) and the tissue parameters (T1 and T2*).

$$S = PD \frac{1 - e^{-TR/T1}}{1 - \cos\theta e^{-TR/T1}} \sin\theta e^{-TE/T2^*} \qquad [4]$$

where S is the image signal intensity, TR is the repetition time, TE is the time to echo, θ is the flip angle, PD is the proton density, T1 is the longitudinal relaxation time, and T2* is the effective transverse relaxation time. However, there are three unknown parameters in Equation [4]; therefore, T1 cannot be directly calculated from a single image. Equation [4] is simplified by incorporating PD and T2* effects into the variable S' (Equation [5]).

$$S = S' \frac{1 - e^{-TR/T1}}{1 - \cos\theta e^{-TR/T1}} \sin\theta \qquad [5]$$

This redefinition step is performed because S' can be approximated so that a pseudo form of T1 images can be calculated.

S' and T1 are the unknown variables in Equation [5]. However, expected T1 values for WM, GM, and CSF are known. Regions of interest (ROIs) are selected to measure the average signal value within WM, GM, and CSF. In addition, S' can be approximated within ROI, using the average signal for a tissue ($\overline{S}_i$) and the expected value of T1 for that tissue ($\overline{T1}_i$). The resulting pseudo form of S'_i is designated S'_{P_i} (Equation 6).

$$S'_{P_i} = \frac{\overline{S}_i (1 - \cos\theta e^{(-TR/\overline{T1}_i)})}{(1 - e^{(-TR/\overline{T1}_i)}) \sin\theta} \approx S'_i \qquad [6]$$

where $\overline{S}_i$ is the average signal value obtained from an ROI placed in the tissue of interest, *i*. $\overline{T1}_i$ is defined as the expected value of T1 for tissue *i*. The expected T1 values for WM, GM, and CSF at 1.5 Tesla are 650, 975, and 3,600 msec, respectively. These expected WM and GM T1 values were based on 19 human T1 studies. Calculated values for CSF were widely variable. Therefore, the target T1 value of 3,600 msec was selected for CSF. This value was considered representative of a normal population, because CSF is water-like (18).

S'_{P_i} is used in Equation [5], in place of S', and is rearranged to calculate T1 using Equation [7]. This approach guarantees that brain tissue signal values map to their expected T1 values. It yields only valid T1 approximations for the targeted tissue. Therefore, T1 values calculated with S'_{P_i} values are designated pseudo-T1 values or $T1_{P_i}$ values, as shown in Equation [7] (r is the voxel index). The mean pixel values of WM, GM, and CSF are mapped to their expected mean T1 values in what are termed WM-, GM-, and CSF-weighted images, when using Equation [7].

$$T1_{P_i}(r) = \frac{-TR}{\ln\left(\frac{S(r) - S'_{P_i}\sin\theta}{S(r)\cos\theta - S'_{P_i}\sin\theta}\right)} \qquad [7]$$

Three $T1_P$ images are calculated from each 3D SPGR image. These images are called tissue-weighted images because of their dependence on S'_{P_i}. Typical signal-to-noise ratios (SNR) for WM and GM in the WM- and GM-weighted images were 21 and 17, respectively. These are better than, but similar to, the WM and GM SNRs (16 and 10) in the phantoms used to develop the FCs.

The T1 FC method uses tissue-weighted T1P images to extract voxel fraction (VF) images. Pixel values in VF_i images are estimators of the fraction of tissue *i* present in the corresponding voxels. The creation of VF_i images is illustrated in Figure 2 and is accomplished in four steps: *(a)* subject normalization, *(b)* segmentation, *(c)* voxel volume correction, and *(d)* classification correction. Each of these steps is discussed in detail below.

Subject Normalization

A standard set of FCs is used with all subjects' images, requiring that image data be adapted to the classifiers, using Equations [6] and [7]. This normalization maps a single tissue class in each 3D SPGR image to the standard reference tissue class in T1 space. WM, GM, and CSF, as defined by the operator, are mapped to the standard reference values of 650, 975, and 3600 msec, respectively.

Subject normalization of each 3D SPGR image data set requires that an operator select three ROIs that are representative of the WM, GM, and CSF. Figure 3 illustrates the recommended locations of ROIs used to designate tissue samples with negligible partial volume averaging. WM, GM, and CSF means from these locations were provided for both accurate and reproducible volume measurements in human and phantom data.

Voxel Volume Correction

Voxel volume correction ensures that the total tissue fraction in each voxel is not greater than unity. A constraint of the FC method is that a voxel can contain at most two tissues, and the total of the tissue fractions must be unity. This is reflected in the FCs that sum to unity for any T1 value (Fig. 1). This requirement holds when VF images are calculated from a single parametric T1 image; ie, three VF images are calculated directly from the same T1 image (15). However, this requirement is often violated when WM, GM, and CSF VF images are calculated from three independent images (WM-, GM- and CSF-weighted T1P images, as shown in Fig. 2), because the corresponding voxels can have different T1 values. To correct for this, corresponding voxels from WM, GM, and

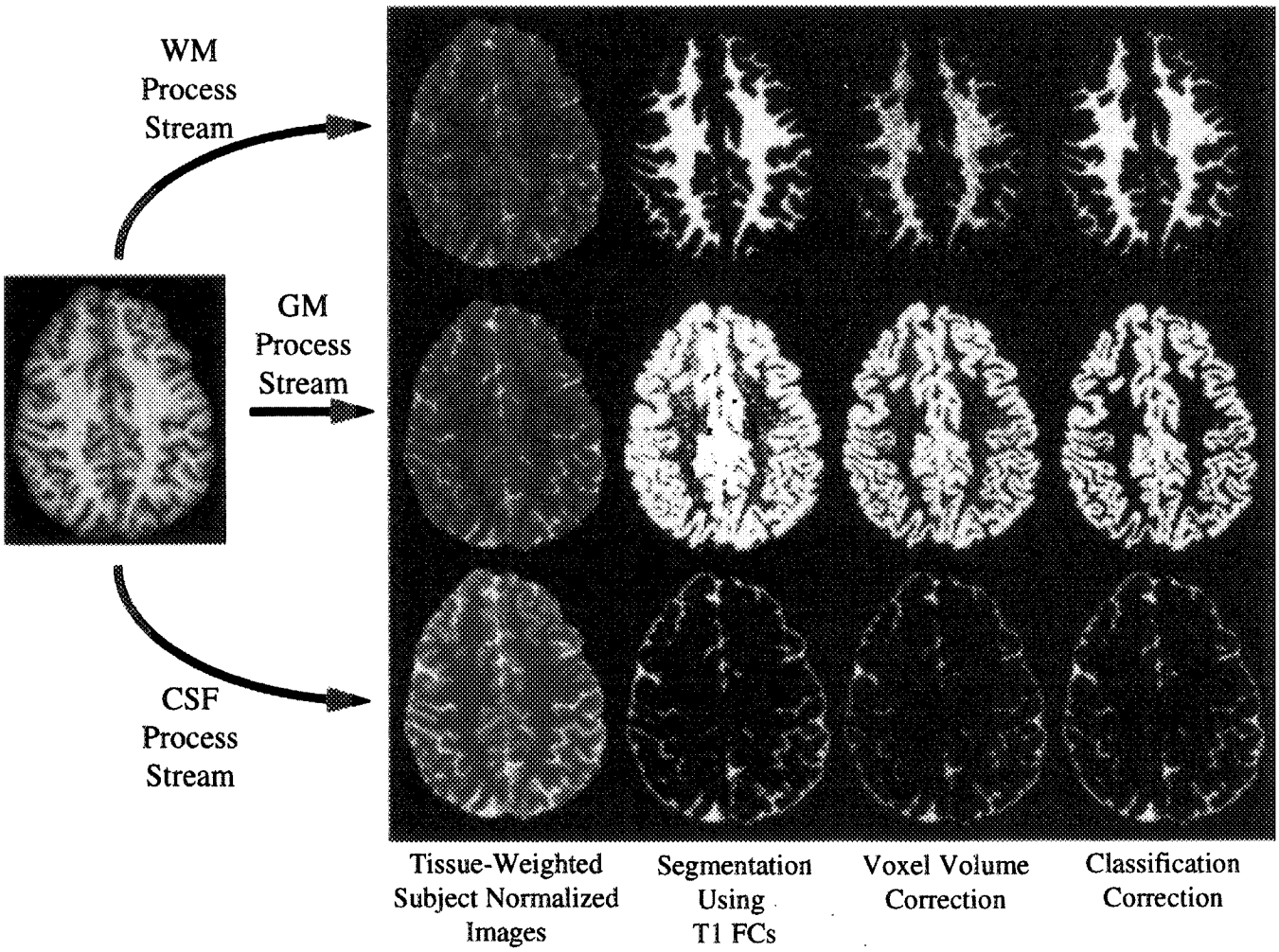

Figure 2. Processing streams for calculating voxel fraction images from 3D SPGR images. **(a)** Subject images are normalized to the standard set of fuzzy classifiers by calculating WM-, GM-, and CSF-weighted images. **(b)** Tissue-weighted images are segmented using the standard fuzzy classifiers (FCs). **(c)** Voxel volume content is corrected so that no voxel contains more than 100% of two tissues. This step reveals the contour of the cortex. **(d)** Tissue misclassifications, many of which are obvious in the segmented images of step **(c)**, are corrected.

CSF VF images, with tissue fractions summing to greater than unity, were normalized to unity.

Classification Correction

WM, GM, and CSF misclassifications commonly occur as a result of this voxel volume normalization step. Obvious misclassifications of GM in known WM regions are apparent in Figure 2 at the voxel volume correction step. Numerous WM-only voxels were misclassified as containing both WM and GM. Reclassification of such WM voxels was accomplished by thresholding the WM VF image. The threshold was selected to ensure that the bulk of misclassified WM voxels were accurately reclassified. Threshold selection can be made from histograms calculated from ROIs placed in the WM images at the voxel volume correction step. These ROIs should be placed away from tissue borders, as illustrated by the oval ROIs in Figure 3. These histograms generally reveal bimodal distributions. The two peaks correspond to voxels filled or partially filled with WM. These partially filled voxels are reclassified to 100% WM by thresholding. An adaptive threshold was not required, because the lower modes were invariably above .5. Preliminary results indicate that a fixed threshold works well with 3D SPGR data acquired from different MR imaging systems with different flip angles. Therefore, this step was implemented automatically, using a threshold of .5, which worked well on all 3D SPGR data acquired from all subjects evaluated.

This thresholding step modified the fuzzy classification of WM by assigning WM voxel fractions above the threshold to unity. All corresponding voxels in the GM VF image are reclassified by setting their voxel fractions to zero to ensure voxel volume normalization. Similarly, voxel values in the CSF VF images above the threshold were reclassified by setting their voxel fractions to unity and the corresponding voxel fractions in the GM VF images to zero.

The steps used to measure WM and GM from 3D SPGR images by the pseudo-T1 method were: *(a)* Perform subject normalization on SPGR images by transforming them into WM-, GM-, and CSF-weighted T1P data. *(b)* Segment WM, GM, and CSF from the subject-normalized T1P data into voxel fraction images, using the standard fuzzy classifiers in Figure 1. Perform *(c)* voxel volume correction and *(d)* classification correction of voxel fraction images. At the beginning of step *a*, an operator obtains mean tissue values from ROIs drawn in the WM, GM, and CSF regions. These mean tissue values are used to calculate

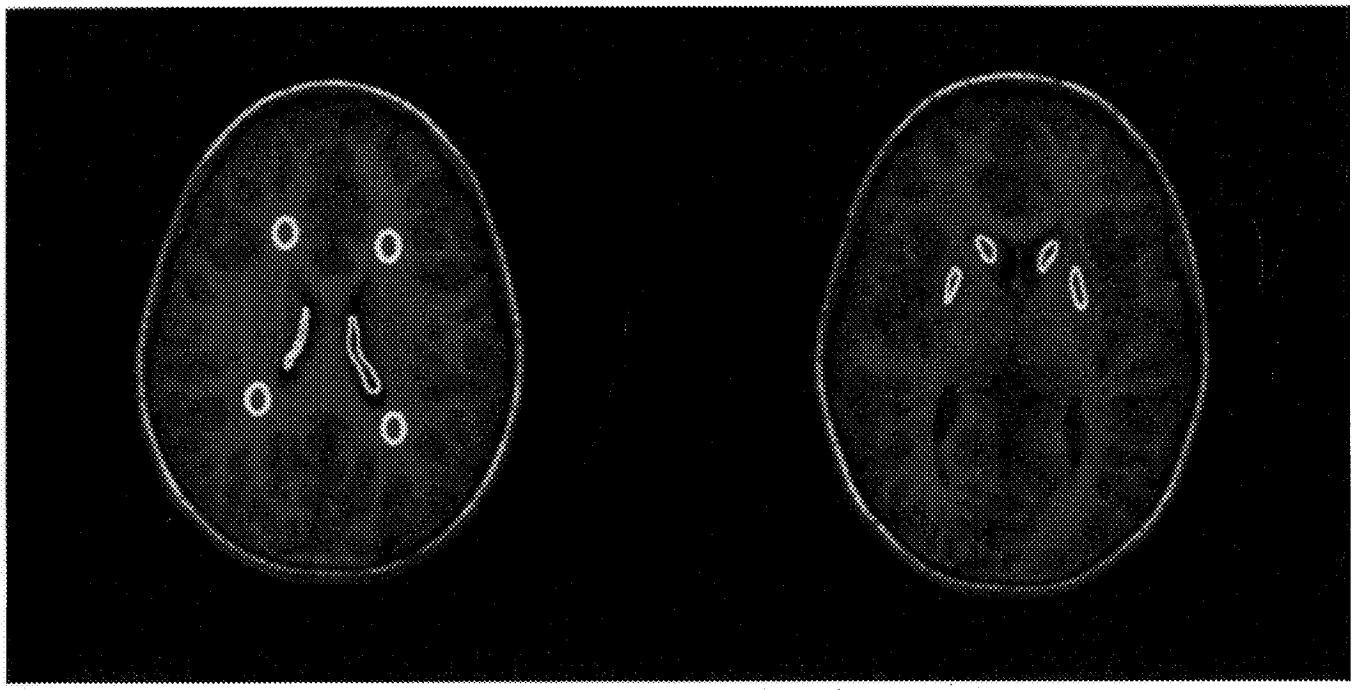

Figure 3. Human brain 3D MR SPGR images. WM and CSF ROIs are illustrated in the axial image containing the ventricles. GM ROIs are placed in the axial image containing the head of the caudate and the putamen.

tissue-weighted images completing the subject normalization step. Steps *b*, *c*, and *d* (segmentation, voxel volume, and classification corrections) were fully automated.

Validation

Three validation techniques were used to test the pseudo-T1 segmentation method. The first approach was to compare volumes calculated from the synthesized phantom images to their known volumes. The second validation technique—calculated from the same human subject—compared the brain tissue volumes obtained by the pseudo-T1 method, as presented in this paper, with the previously published T1 method (15). Finally, GM/WM ratios calculated from MR data were compared with the GM/WM ratios calculated from anatomical data.

Phantoms simulating 3D SPGR images from the superior, middle, and inferior regions of the cerebrum were developed by previously described procedures for T1 phantoms (15). These phantoms were created from human cryosection brain images to ensure anatomical realism. Three sets of 3D SPGR phantom images (with low, mid, and high signal values) were developed to test the segmentation method across the full range of human 3D SPGR data acquired from 34 normal subjects. Intrinsic WM, GM, and CSF inhomogeneities were modeled in each phantom image set by filling tissue ROIs with mean tissue signal values and zero-mean gaussian noise corresponding to tissue measurements collected from human image data (low, mid, and high signal values). Partial volume averaging effects were modeled in the *x*, *y*, and *z* directions as previously detailed (15). These 3D SPGR phantoms were used to evaluate volume measurements by the new FC method over a wide range of expected imaging conditions.

T1-weighted image data sets were acquired on a GE 1.5 Tesla Signa scanner using a 3D SPGR pulse sequence. The pulse sequence was a volume acquisition, with TE = 5 msec, TR = 24 msec, flip angle = 45°, and one excitation. Each acquisition contained 128 256 × 256 images with 24-cm fields of view and 1.5-mm-thick slices. Nonbrain tissues were segmented from the 3D SPGR image data sets, using a semiautomatic algorithm, before application of the FC method. Manual editing was used to remove nonbrain tissues that had voxel values similar to brain voxel values, eg, where the optic nerves connect to the brain.

WM and GM volume measurements were made from the same person, using the pseudo-T1 method presented in this paper and the previously published T1 method (15). The pseudo-T1 method used images acquired with the 3D acquisition protocol. The T1 method used a conventional spin-echo protocol to calculate T1 images. The 256 × 256 MR images used to calculate T1 parametric images were also acquired with a GE Signa 1.5-T MR imager. The slices were 5-mm thick with a 1.5-mm gap and a 24-cm field of view. The spin-echo acquisition protocol was TE = 20, TR = 500 for T1W images, and TE = 30 and 80 with TR = 2,400 for the DE images.

The fuzzy segmentation software was written as a C-coded module within the Digital Imaging Processing Station (DIPS) version 1.6 software package (Hayden Image Processing Group, Boulder, CO). WM or GM images were subject normalized and segmented from 256 × 256 3D SPGR images in approximately 15 seconds on a Macintosh Quadra 840AV. This Quadra 840AV uses a Motorola 68040 microprocessor running at 40 MHz and has 32 megabytes of RAM.

• RESULTS AND DISCUSSION

The pseudo-T1 segmentation method presented in this paper was validated with three sets of phantoms. These phantom image sets (low, mid, and high signal values) were chosen to test the method's adaptability to signal variations across a population. In addition, this method was tested by comparing volume measurements from the same subject as scanned by two different protocols and segmentation methods. A final validation was performed by comparing human WM and GM volumes measured

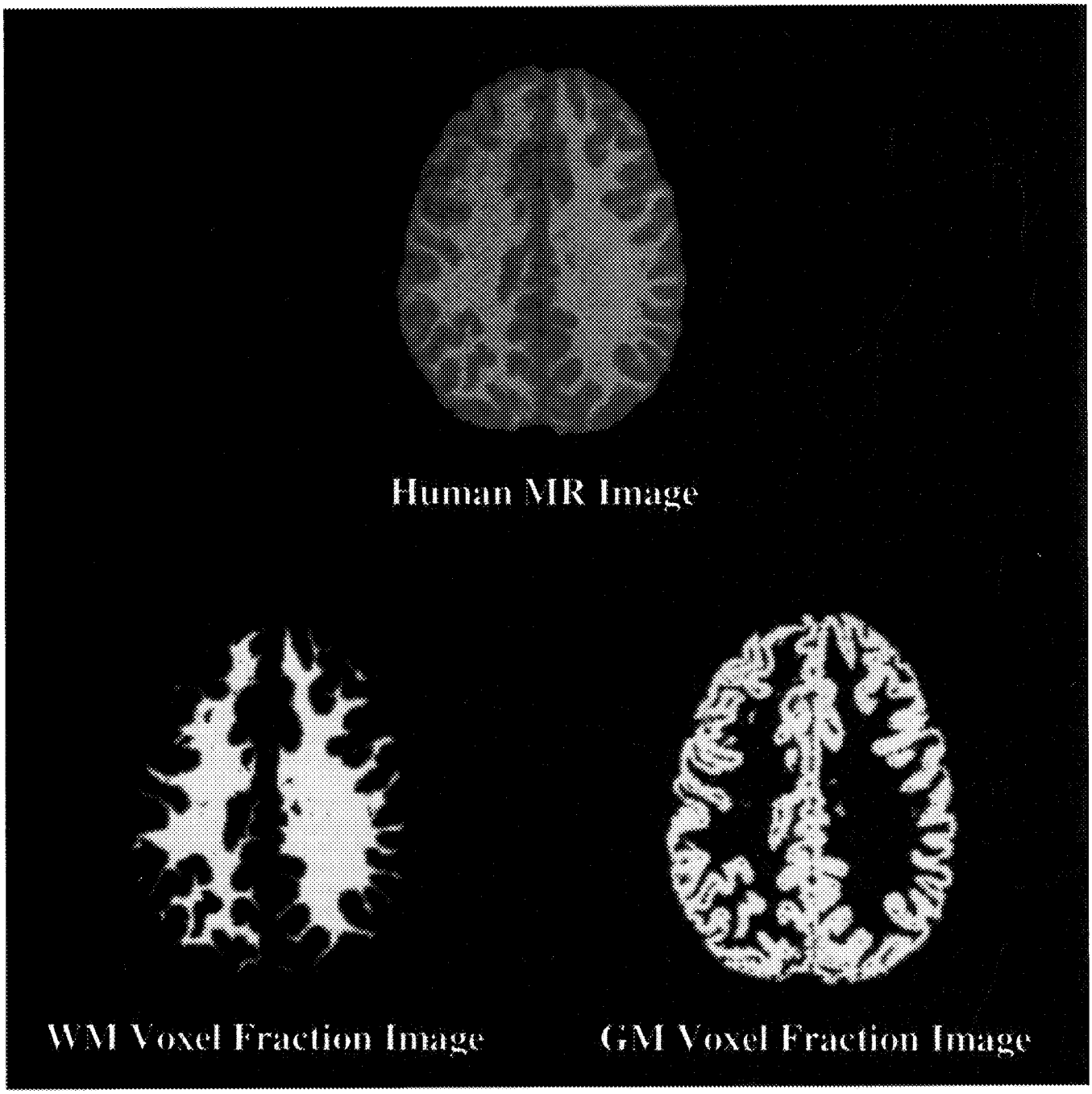

Figure 4. 3D human MR image with WM and GM voxel fraction images.

from MR images to volumes measured from anatomical data. These human MR data sets were selected because they represented the extent of signal variation in our population.

The previously described method used to calculate the T1 parametric images for the T1 FC method requires three sets of nonparametric images (T1W, T2W, and PDW) (15). In contrast, the pseudo-T1 FC method presented in this paper is based on a single nonparametric image, although three intermediate images (WM-, GM-, and CSF-weighted images) were synthesized to produce VF images. WM and GM VF images were calculated from human and phantom 3D SPGR images. Samples of these human and phantom 3D SPGR images, along with their VF images, are shown in Figures 4 and 5. The 3D SPGR phantom image is shown to illustrate the similarity between the 3D SPGR phantom and human images. The segmented human WM and GM images are qualitatively appealing and quantitatively accurate, as determined by results from phantom volume measurements.

Phantom volume measurements show the average relative error as approximately 2% for WM and 3% for GM (Table 2). Relative errors overall were slightly higher in the superior slices than in the inferior and middle slices. This difference probably results from the increased partial volume averaging between WM and GM in the superior regions of the brain. Notably, errors due to partial volume averaging along the edges of the ventricles were automatically reduced in the middle and inferior slices by the classification correction step. Partial volume-averaged WM and CSF voxels appear as GM voxels at the ventricle edges. Many of these misclassified GM voxels

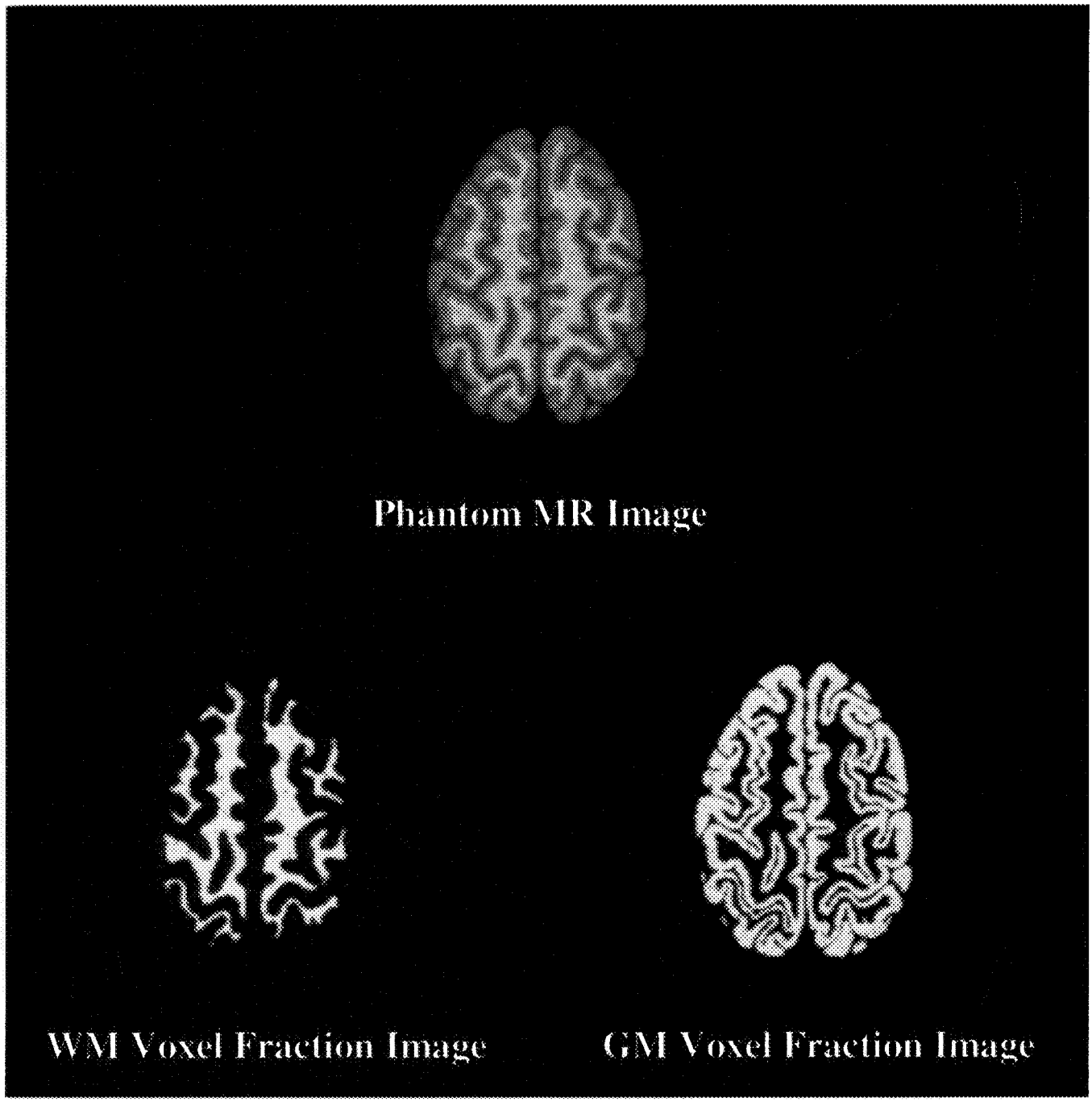

Figure 5. 3D phantom MR image with WM and GM voxel fraction images.

are reclassified into WM and CSF voxels during step 4 of processing. Phantom volume measurements were accurate for different slices as well as for different signal values (Table 2). Absolute volume errors, on a slice-by-slice basis, were generally less than 0.2 cm^3 for WM and 0.4 cm^3 for GM. GM error rates are slightly higher, because GM partial volume averages extensively with WM and CSF, whereas, predominately, WM partial volume averages only with GM.

GM/WM volume measurements obtained from the same person by the T1 (spin-echo data) method were 646 cm^3/347 cm^3 (= 1.86) and for the pseudo-T1 (3D data) method were 625 cm^3/352 cm^3 (= 1.78). GM and WM volumes measured from the 3D images were 3.3% smaller and 1.4% larger, respectively, than GM and WM volumes measured from the T1 images. This analysis shows that the pseudo-T1 method can make volume measurements that compare well with the those obtained by the previously published T1 method. In addition, it demonstrates the utility of applying the FCs to either T1 parametric or T1W nonparametric 3D SPGR MR images. This GM/WM comparison also illustrates the accuracy of FC modeling of partial volume averaging effects between images with greatly differing voxel volumes (due to differences in slice thickness).

Two important points relating to operator interactions are emphasized. The first point is that tissue samples taken by an operator from adjacent slices were consistently within 5% of each other. This level of variation in $\bar{S}_i$ showed little effect on the measurement accuracy. Sec-

Table 2
True and Calculated Gray Matter and White Matter Volumes in 1.5-mm Thick 3D SPGR Phantom Images

Slice Location	White Matter				Gray Matter			
	True Volume	Low Signal Phantom	Mid Signal Phantom	High Signal Phantom	True Volume	Low Signal Phantom	Mid Signal Phantom	High Signal Phantom
Superior	4.6	5.0	4.7	4.7	10.0	9.9	10.0	10.2
Middle	18.2	18.3	18.1	18.0	13.6	14.0	14.1	14.5
Inferior	16.2	16.6	16.2	16.1	18.4	18.5	18.8	19.2
Total	39.0	39.9	39.0	38.8	42.0	42.4	42.9	43.9

Note.—All volume measurements are in cubic centimeters. Phantom data sets simulate normalized human 3D SPGR MR data with low, medium, and high signal values from a pool of 34 data sets.

ond, it was common to find subjects with constricted ventricles, making the ROI placement more difficult and partial volume averaging errors likely. Careful examination of the ventricles was required to choose a good location for the CSF ROI. Usually, CSF ROIs contained 50 to 150 voxels. Tissue homogeneity was assessed by standard deviation determined from the tissue ROI. Typical relative standard deviations within WM, GM, and CSF ROIs, were 4.8%, 5.7%, and 21.7%, respectively.

This pseudo-T1 segmentation method was designed to adapt to image intensity variations due to partial volume averaging and intrinsic tissue inhomogeneities in a normal population. Variations in pixel values attributable to RF nonuniformities were not directly modeled. However, the ability of the method to accommodate shading artifacts was examined. WM measurements from 34 subjects revealed that, on average, signal intensity values varied by 2.4% from left to right and by 1.8% from anterior to posterior. Measurements were gathered from four WM ROIs placed immediately superior to the ventricles. Two were placed in each hemisphere and were separated as much as possible. WM was chosen because it had large regions (this ensured that only WM was sampled) in both hemispheres and in the anterior and posterior portions of the image. WM measurements made from this slice location were assumed to be representative of the bulk of cerebral WM. Most important, the comparison between the volume measurements, acquired from the same individual by both the T1 method and the pseudo-T1 method provided favorable quantitative evidence that the shading artifacts encountered in the 3D SPGR image data had minimal adverse effects on the segmentation. The pseudo-T1 method was designed to adapt to signal variations that were primarily the result of intrinsic variations in human subjects and partial volume averaging effects. The results indicated that small local and global variations from other effects were also well accommodated by the pseudo-T1 method.

The 3D SPGR pulse sequence used in this research was selected by clinicians because it provided good WM/GM contrast. This method is not tailored to a specific SPGR protocol or even to the SPGR pulse sequence itself. The original goal of this research was to apply the pseudo-T1 method to T1W MR images acquired from different protocols. The pseudo-T1 method will not work well with the aggregate of T1W MR protocols. However, it does work well with thinly sliced images because of their reduced partial volume averaging. The correction steps, illustrated in Figure 2, compensated for tissue classification errors in the segmented tissue images, in large part, because of this minimized partial volume averaging. Preliminary segmentation results from SPGR images acquired with different flip angles indicate that it may work well with a significant subset of thin-sliced T1W MR protocols.

The final validation of the pseudo-T1 method was a comparison of volume measurements acquired from MR data with those acquired from anatomical data. Cerebral GM and WM volumes were estimated from human anatomical data. Combining whole brain and cerebral cortex volumes of approximately 1,400 and 700 cm^3 with estimates of cortex and WM at 83% and deep GM structures (putamen, globus pallidus, caudate nucleus, diencephalon, and mesencephalon) at 5% produces the average values of 770 and 462 cm^3 for GM and WM (19,20). Cerebral GM and WM volumes from four human 3D SPGR data sets were 625, 763, 728, and 731 cm^3 and 352, 476, 381, and 395 cm^3, respectively. The average cerebral GM/WM ratio for these four SPGR data sets is 1.77; the ratio estimated from average anatomical data is 1.67. GM/WM ratios measured from phantom images were generally within a few percent of the true GM/WM ratios (10.0 cm^3/4.6 cm^3 = 2.17, 13.6 cm^3/18.2 cm^3 = 0.75, and 18.4 cm^3/16.2 cm^3 = 1.14 for superior, middle, and inferior phantoms).

The GM/WM ratios calculated from the 3D SPGR data and from the anatomical data are much larger than the near unity GM/WM ratios reported by Kikinis et al and Rusinek et al (4,10). The fuzzy classification method presented in this paper directly models both the intrinsic inhomogeneity of tissues and the partial volume averaging that occurs between tissues. We believe that the incorporation of these natural features into our segmentation method accounts, in large part, for the difference between the 1.77 GM/WM ratio and the near unity ratios previously reported.

Conclusions

A fuzzy segmentation method, developed for T1 images, was modified for use with T1-weighted 3D MR images. The method was validated by using brain phantom data sets derived from cryosection images of a human brain. The pseudo-T1 method was also validated by direct comparison with the previously published T1 method. In addition, it was validated by comparison with anatomical data. These validations emphasize that this segmentation method is an accurate and precise tool for extracting WM and GM volumes from T1-weighted 3D MR images of the human brain.

References

1. Vannier MW, Butterfield RL, Jordan D, et al. Multispectral analysis of magnetic resonance images. Radiology 1985; 154: 221–224.
2. Cline HE, Lorenson WE, Kikinis R, Jolesz F. Three-dimensional segmentation of MR images of the head using probability and connectivity. J Comput Assist Tomogr 1990; 14:1037–1045.
3. Kohn MI, Tanna NK, Herman GT, et al. Analysis of brain and cerebrospinal fluid volumes with MR imaging. Part I: methods, reliability, and validation. Radiology 1991; 178:115–122.
4. Kikinis R, Shenton ME, Gerig G, et al. Routine quantitative analysis of brain and cerebrospinal fluid spaces with MR imaging. J Magn Reson Imaging 1992; 2:619–629.
5. Bonar DC, Schaper KA, Anderson JR, Rottenberg DA, Strother SC. Graphical analysis of MR feature space for measurement

of CSF, gray-matter, and white-matter volumes. J Comput Assist Tomogr 1993; 17(3):461–470.
6. Fletcher LM, Barsotti JB, Hornak JP. A multispectral analysis of brain tissues. Magn Reson Med 1993; 29:623–630.
7. Jackson EF, Narayana PA, Falconer JC. Reproducibility of nonparametric feature map segmentation for determination of normal human intercranial volumes with MR imaging data. J Magn Reson Imaging 1994; 4:692–700.
8. Kao Y, Sorenson JA, Bahn MM, Winkler SS. Dual-echo MRI segmentation using vector decomposition and probability techniques: a two-tissue model. Magn Reson Med 1994; 32:342–357.
9. Brandt MR, Bohan TP, Kramer LA, Fletcher JM. Estimation of CSF, white and gray matter volumes in hydrocephalic children using fuzzy clustering of MR images. Comp Med Imaging Graph 1994; 18:25–34.
10. Rusinek H, de Leon MJ, George AE, et al. Alzheimer disease: measuring loss of cerebral gray matter with MR imaging. Radiology 1991; 178:109–114.
11. Hillman GR, Kent TA, Kaye A, et al. Measurement of brain compartment volumes in MR using voxel composition calculations. J Comput Assist Tomogr 1991; 15(4):640–646.
12. DeCarli C, Maisog J, Murphy DGM, et al. Method for quantification of brain, ventricular, and subarachnoid CSF volumes from MR images. J Comput Assist Tomogr 1992; 16(2): 274–284.
13. Gage HD, Santago P, Snyder WE. Quantification of brain tissue through incorporation of partial volume effects. SPIE, Medical Imaging VI: Image Processing 1992; 1652:84–96.
14. Peck DJ, Windham JP, Soltanian-Zadeh H, Roebuck JR. A fast and accurate algorithm for volume determination in MRI. Med Phys 1992; 19:599–605.
15. Herndon RC, Lancaster JL, Toga AW, Fox PT. Quantification of white matter and gray matter volumes from T1 parametric images using fuzzy classifiers. J Magn Reson Imaging 1996;6: 425–435.
16. Clarke LP, Velthuizen RP, Camacho MA, et al. MRI segmentation: methods and applications. Magn Reson Imaging 1995; 13(3):343–368.
17. Wehrli F. Fast scan magnetic resonance imaging. New York: Raven, 1991.
18. Fullerton GD. Physiologic Basis of Magnetic Relaxation. In: Stark DD, Bradley WG, eds. Magnetic resonance imaging. St. Louis: Mosby, 1992; 88–108.
19. Carpenter, MB. Core text of neuroanatomy. Baltimore: Williams & Wilkins, 1985.
20. Blinkov SM, Glezer II. The human brain in figures and tables. New York: Basic Books, 1968.